



RESIDENT AND MEDICAL STUDENT SECTION

SIO RMSS Research Digest - November 2025

In 2025, the Society of Interventional Radiology (SIR) featured its [annual list](#) of “Top Paper Awards,” chosen amongst articles published in the Journal of Vascular and Interventional Radiology (JVIR) in 2024.

In this second research digest brought to you by the Society of Interventional Oncology (SIO) Resident and Medical Student Section (RMSS), we summarize and discuss several of these awarded manuscripts related to interventional oncology, in order to help readers unpack these studies and integrate important findings/takeaways into their practice.

This research digest is brought to you by research digest authors and RMSS research subcommittee members Chris Hsu, Connor Centner, Katrina Falk, Madelon Dijkstra, Omid Shafaat, Salma Abosabie, Setayesh Sotoudehnia Korani, and Travis Pebror; by digest editor and RMSS resident co-chair Gabriel Knight MD; and by digest editor and RMSS faculty advisor Julia D’Souza MD.

If you have not already, please also check out our [inaugural research digest](#), in which we summarized and contextualized six landmark manuscripts within the field of interventional oncology discussed during the “Must-Know Papers” session at the Society of Interventional Oncology (SIO) 2025 Annual Scientific Meeting.

Paper #1: Measurement of the Tumor-to-Normal Ratio for Radioembolization of Hepatocellular Carcinoma: A Prospective Study Comparing 2-Dimensional Perfusion Angiography, Technetium-99m Macroaggregated Albumin, and Yttrium-90 SPECT/CT (Brunson et al.) [<https://doi.org/10.1016/j.jvir.2023.09.023>]

RMSS Author: Connor Centner

RMSS Editors: Gabriel Knight, Julia D'Souza

SUMMARY (METHODS, RESULTS):

This prospective single-arm study enrolled 15 participants with hepatocellular carcinoma (HCC) scheduled for transarterial radioembolization (TARE) and **compared tumor-to-normal (T:N) ratios derived from 2D perfusion angiography with those obtained from technetium-99m macroaggregated albumin (99mTc-MAA) SPECT/CT and post-yttrium-90 (Y-90) bremsstrahlung SPECT/CT**. Ultimately, the authors sought to investigate **whether 2D perfusion angiography could be used to simplify treatment planning compared to the traditional 99mTc-MAA/nuclear medicine approach**.

All patients received segmental treatment with glass microspheres; the mean dose to tumor was 918.9 Gy (SD \pm 656.0), whereas it was 495.1 Gy (SD \pm 325.0) to normal liver. 2D arteriograms were analyzed using the included Perfusion acquisition mode as part of the Azurion ClarityIQ angiographic system (Philips, Amsterdam, Netherlands) employed by the operators.

There was **no significant difference between T:N calculations between 99mTc-MAA SPECT/CT and 2D perfusion angiography (2.28 ± 0.89 vs 2.25 ± 0.99 , $p = 0.45$)**, with a weak positive correlation between two methods (Pearson correlation coefficient = 0.28). Among the 13 patients who underwent TARE, the T:N ratio from 2D perfusion angiography was also not significantly different from that derived from post-Y-90 SPECT/CT (2.25 ± 1.05 vs 1.91 ± 0.39 ; $P = 0.12$) with a weak positive correlation (Pearson correlation coefficient = 0.26). **Both 2D perfusion angiography and 99mTc-MAA appeared to similarly overestimate the realized post-treatment T:N ratio**. Of the 12 evaluable patients, 8 (67%) achieved complete response and 4 (33%) partial response by modified Response Evaluation Criteria in Solid Tumors criteria.

Key Findings:

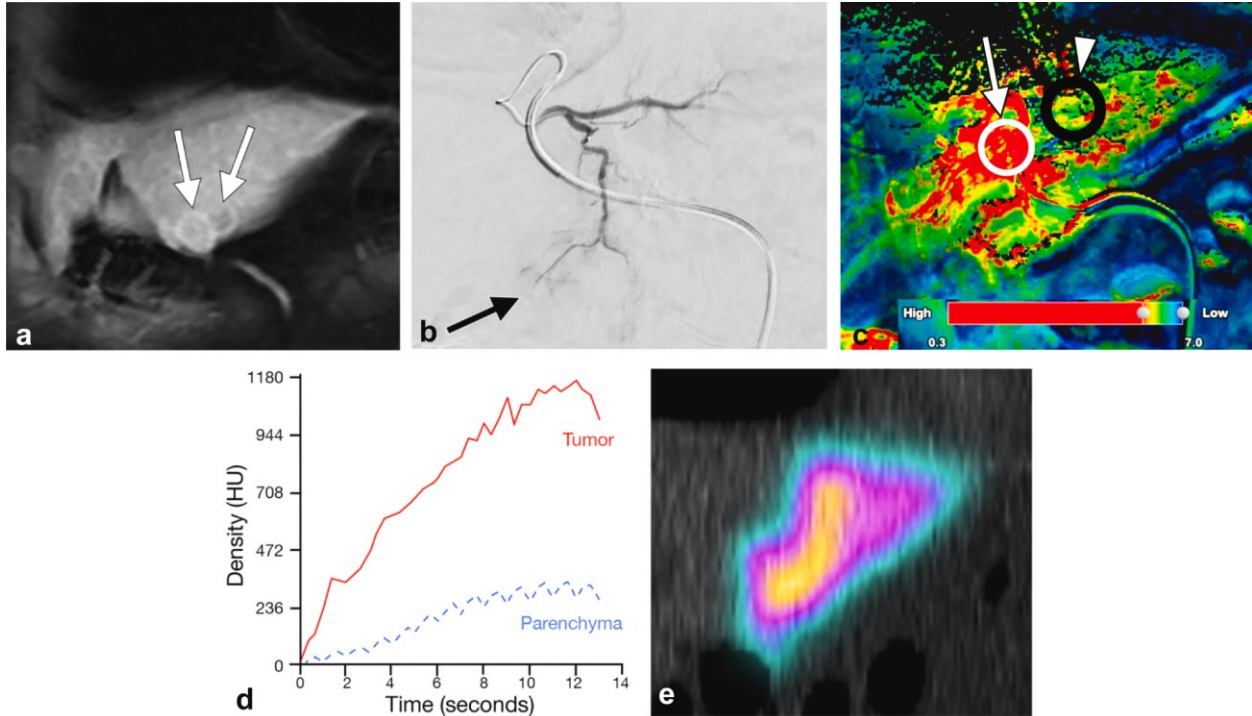
- **2D perfusion angiography performs similarly to 99mTc-MAA for T:N estimation.** T:N ratios derived from 2D perfusion angiography were statistically comparable to those from 99mTc-MAA SPECT/CT (2.25 vs. 2.28 , $p = 0.45$) with a moderately-positive correlation ($r = 0.28$).

- **Both pre-treatment methods overestimate post-treatment Y-90 T:N ratios.** When compared with post-Y-90 bremsstrahlung SPECT/CT, both 2D perfusion angiography and MAA overestimated delivered dose distribution, indicating **limitations in predicting actual microsphere deposition and dose heterogeneity.**
- High objective response rate following TARE. Among evaluable patients, 67% achieved complete response and 33% partial response, demonstrating efficacy of segmental TARE in this cohort.

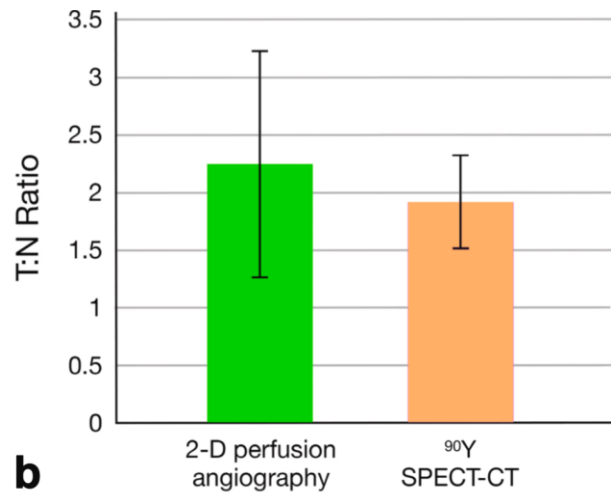
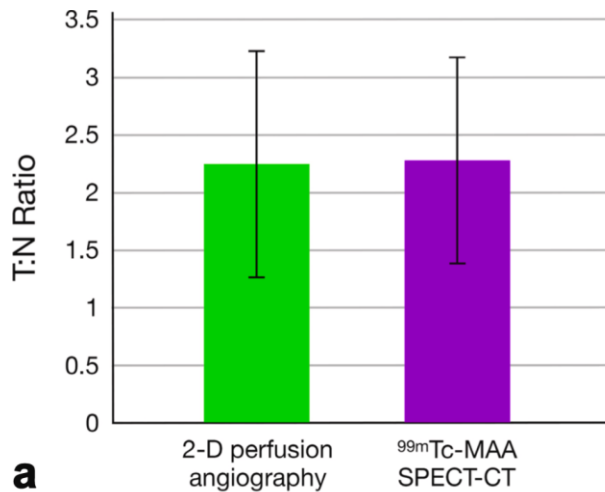
IMPORTANT TAKEAWAYS/DISCUSSION:

- **2D perfusion angiography may be a viable alternative to mTc-MAA for pre-TARE shunt evaluation.** Since T:N estimation closely mirrors MAA, 2D perfusion angiography could **offer immediate hemodynamic information without needing additional nuclear imaging, supporting its potential role for real-time treatment planning or catheter optimization.**
 - **Critically, 2D perfusion angiography does not replace Tc-99m MAA for lung shunt fraction.** The authors state that recent data have suggested that lung shunt fraction calculation is not needed in certain patients with HCC undergoing TARE, but that dosing using the T:N ratio may still be of benefit.
- **The consistent overestimation of T:N across both methods underscores an unmet need for more accurate predictors of microsphere deposition.**
- Despite predictive limitations, sufficient complete and partial responses occurred following segmental TARE.
- **In patients with small HCCs within Milan criteria who are likely to exhibit negligible LSFs, 2D perfusion angiography may provide a facile alternate to 99mTc MAA-based dosimetry** and may be of particular use in centers already practicing same-day planning and 90Y administration who wish to incorporate advanced dosimetry in their treatments.

KEY FIGURES:



(a) Coronal arterial phase magnetic resonance (MR) imaging of the abdomen demonstrated a segment III hepatocellular carcinoma (HCC; arrows). (b) Digital subtraction angiogram with the tip of the microcatheter positioned within the proximal segment III artery. Tumor enhancement was seen distal to the catheter (black arrow). (c) 2D perfusion arteriogram with the microcatheter in the proximal segment III artery demonstrated a focus of increased density and perfusion (white arrow and circle) within segment III, corresponding to the segment III tumor as seen on the MR image with decreased perfusion in the adjacent parenchyma (arrowhead and black circle). (d) Time–density curve corresponding to the 2D perfusion arteriogram; the solid curve represents the tumor region of interest (ROI), and the dotted curve corresponds to the adjacent normal segment III parenchyma ROI. (e) Coronal ^{99m}Tc MAA single-photon emission computed tomography (SPECT)/CT demonstrated high uptake in the segment III tumor and adjacent parenchyma. CT = computed tomography; MAA = macroaggregated albumin; ^{99m}Tc = technetium-99m.



(a) Tumor-to-normal (T:N) ratio calculated by 2D perfusion angiography vs ^{99m}Tc MAA SPECT/CT (2.28 [SD ± 0.89] vs 2.25 [SD ± 0.99]; P = .45). (b) The T:N ratio calculated by 2D perfusion angiography vs post-TARE ⁹⁰Y SPECT/CT (2.25 [SD ± 1.1] vs 1.91 [SD ± 0.15]; P = .12). CT = computed tomography; MAA = macroaggregated albumin; SPECT = single photon emission computed tomography; TARE = transarterial radioembolization; ^{99m}Tc = technetium-99m.

Paper #2: Predictive Dosimetry and Outcomes of Hepatocellular Carcinoma Treated by Yttrium-90 Resin Microsphere Radioembolization: A Retrospective Analysis Using Technetium-99m Macroaggregated Albumin SPECT/CT and Planning Software. (Doyle et al.) [<https://doi.org/10.1016/j.jvir.2023.11.026>]

RMSS Author: Madelon Dijkstra

RMSS Editors: Gabriel Knight, Julia D'Souza

SUMMARY (METHODS, RESULTS):

- Yttrium-90 (Y90) radioembolization is a cornerstone locoregional therapy for hepatocellular carcinoma (HCC), yet **optimal dosing - particularly for resin microspheres - has remained less clearly defined than for glass microspheres**. Historically, many centers relied on body surface area (BSA)–based activity calculations, a blunt tool that ignores true liver treatment volumes and heterogeneous tumor uptake. This study directly addresses a practical and clinically relevant question: **What absorbed tumor dose predicts meaningful tumor response when using resin microspheres, and can pretreatment dosimetry be used to achieve that dose?**
- This was a single-center, retrospective analysis of 101 patients (102 treatments, 127 index tumors) with HCC treated with Y90 resin microspheres between 2015 and 2022. All patients underwent standard mapping angiography with technetium-99m macroaggregated albumin (99mTc-MAA) SPECT/CT, which was then analyzed with commercially-available dosimetry software (SurePlan LiverY90; MIM Software, Cleveland, Ohio) using partition modeling. Tumor response was assessed on serial contrast-enhanced CT or MRI every 2–3 months using mRECIST criteria, with a median imaging follow-up time of 148 days. Objective response (OR) was defined as complete or partial response of the treated index tumor. Most patients had Child-Pugh A liver function (80.4%), BCLC B or C disease (44.1%), and underwent either lobar (55.9%) or segmental (44.1%) treatments using either BSA-based or partition-modeled activity prescriptions.
- Using pretreatment 99mTc-MAA SPECT/CT fused with anatomic imaging, the authors estimated mean absorbed tumor dose (ADT) via a multicompartment partition model. Compartments included tumor, treated liver, untreated liver, and lungs. Importantly, this analysis reflects *predicted* tumor dose from mapping—not post-therapy imaging, which would show true dose delivered.
- The **main result was finding a clear dose–response relationship**.

Key Findings:

- **Tumors that achieved objective response received significantly higher ADT than nonresponding tumors** (median ~142 Gy vs ~71 Gy).
- On multivariable Cox analysis, **ADT was the only factor independently predictive of objective response, outperforming clinical stage, liver function, treatment level (i.e. lobar vs. segmental), and dosimetry method.**
- Regarding durability, **higher ADT was also associated with improved progression-free survival (PFS).** An ADT of 157 Gy corresponded to approximately 92% 1-year PFS. While ADT itself was not independently predictive of progression in all models, **partition modeling (vs BSA) and higher delivered activity were associated with improved PFS.**
- Notably, **partition-modeled treatments achieved substantially higher tumor doses than BSA-based treatments, reinforcing the limitations of BSA dosing.**
- For glass microspheres, prior work has established dose thresholds (e.g., ≥ 205 Gy for lobar treatments, ≥ 400 Gy for segmentectomy) associated with improved outcomes. Comparable thresholds for resin microspheres have been less consistent. This study strengthens emerging evidence suggesting that **tumor doses in the 140–160 Gy range are clinically meaningful for resin microspheres**, aligning with prior retrospective analyses and international expert recommendations that propose minimum targets around 120 Gy. Importantly, the study emphasizes predictive dosimetry—using mapping studies to plan therapy—rather than retrospective dose estimation after treatment. This is a key distinction for clinical decision-making and planning.
- As a retrospective, single-center study, the findings are subject to selection bias and limited by relatively short imaging follow-up. ^{99m}Tc -MAA remains an imperfect surrogate for Y90 microsphere distribution, and only mean tumor dose (not voxel-level heterogeneity) was assessed. The sample size at very high doses (>200 Gy) was small, contributing to wide confidence intervals. Nonetheless, sensitivity analyses supported the primary conclusions.

IMPORTANT TAKEAWAYS/DISCUSSION:

- For Y90 resin microsphere radioembolization, **absorbed tumor dose was stronger predictor of response** than traditional clinical variables.
- **BSA-based dosing often underdoses tumors; partition modeling more reliably achieves therapeutic tumor doses.**
- An estimated tumor dose around 150–160 Gy appears to be a meaningful planning goal when safe from a liver tolerance standpoint.

- These data support prospective, dosimetry-driven Y90 planning and help move resin microsphere therapy toward the same level of personalization already adopted with glass microspheres.

KEY FIGURES:

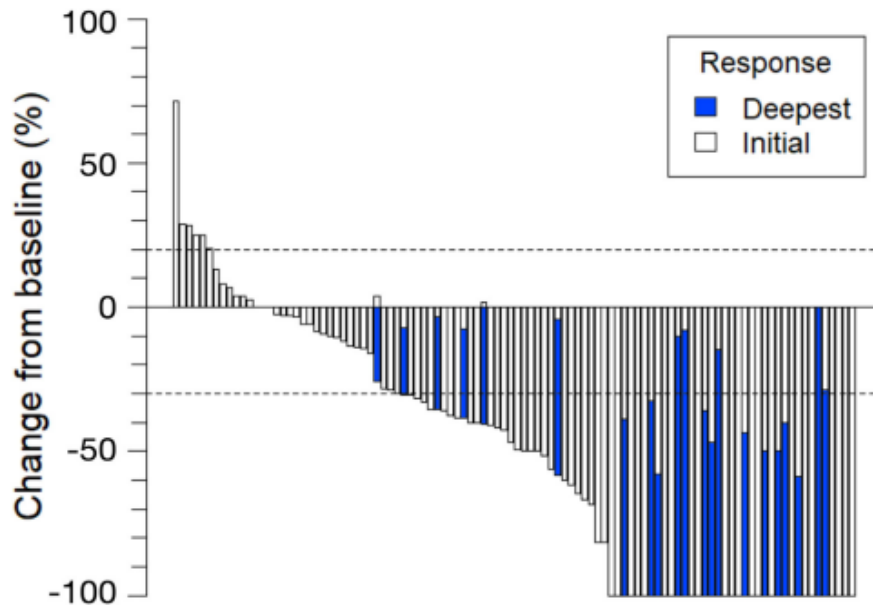


Figure 2. Waterfall plot of tumor response at the best response (shaded) and initial response (white). Each bar represents a treatment. Solid white bars indicate no further modified Response Evaluation Criteria in Solid Tumors (mRECIST) response improvement after initial follow-up. Horizontal dashed lines represent cutoffs for progressive disease at 20% growth and partial response at 30% reduction in size.

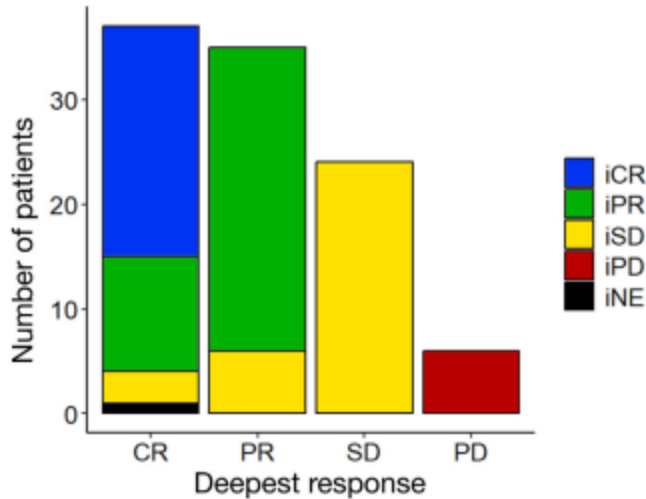


Figure 3. Stacked bar chart representing the best response of treatments. Shading represents the initial response of treatments. There were 22 of 102 (22%) iCR, 40 of 102 (39%) iPR, 33 of 102 (32%) iSD, 6 of 102 (6%) iPD, and 1 of 102 (1%) iNE cases. CR = complete response; iCR = initial complete response; PR = partial response; iPR = initial partial response; SD = stable disease; iSD = initial stable disease; PD = progressive disease; iPD = initial progressive disease; iNE = initially nonevaluable.

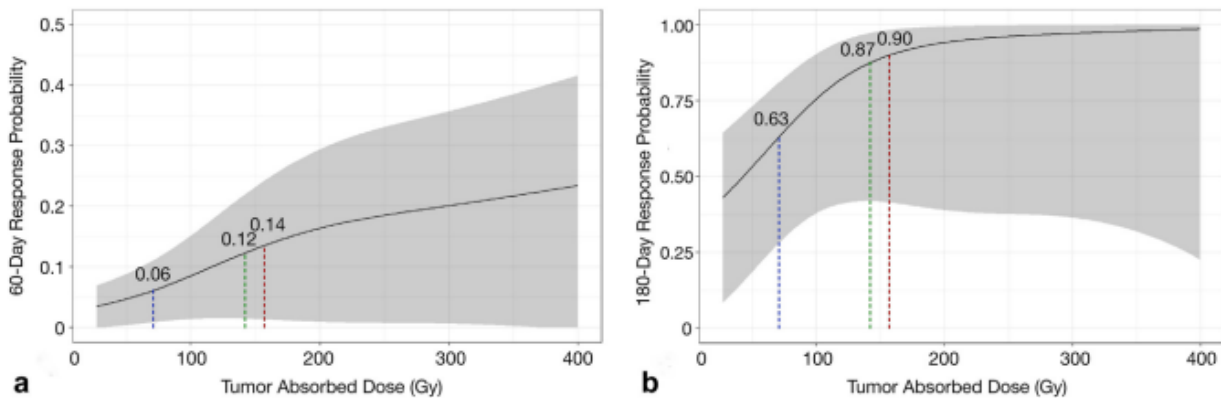


Figure 4. The probability (95% confidence interval [gray]) of objective response by AD_T at (a) 2-month and (b) 6-month follow-ups. Probability was evaluated at AD_T of 70.8 (left line), 142 (middle line), and 157 Gy (right line). Covariates were adjusted at either median values or the most common parameter category. These included male sex, Child-Pugh Class A, Barcelona Clinic Liver Cancer Class B, TNR of 5.25, lobar treatment level, 1 index tumor, and a delivered activity of 1.2 GBq. AD_T = estimated mean absorbed tumor dose; TNR = tumor-to-normal whole liver ratio.

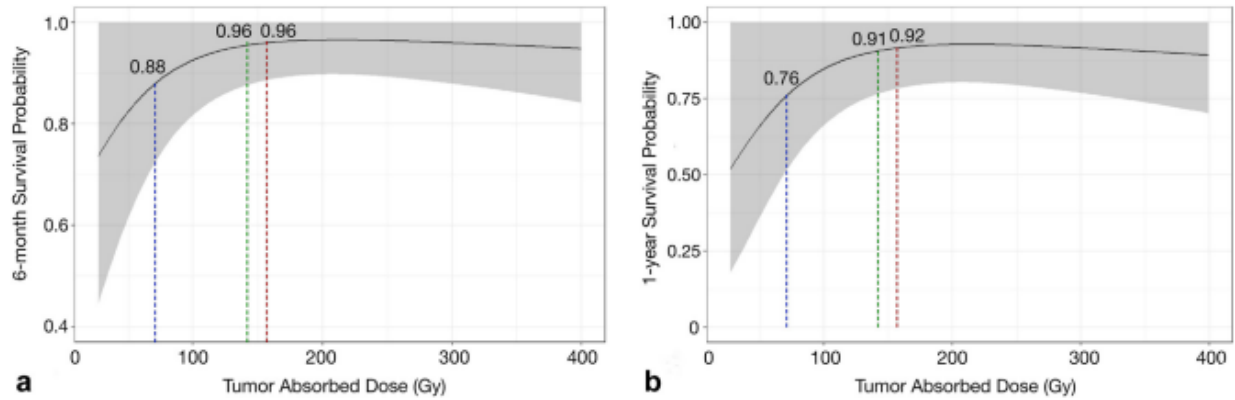


Figure 5. The probability (95% confidence interval [gray]) of PFS by AD_T at **(a)** 6 months and **(b)** 1 year from day of treatment. Probability was evaluated at AD_T of 70.8 (left line), 142 (middle line), and 157 Gy (right line). Covariates were adjusted at either median values or the most common parameter category. These included male sex, Child-Pugh Class A, Barcelona Clinic Liver Cancer Class B, TNR of 5.25, lobar treatment level, 1 index tumor, and a delivered activity of 1.2 GBq. AD_T = estimated mean absorbed tumor dose; TNR = tumor-to-normal whole liver ratio.

Paper #3: Radiation Major Hepatectomy Using Ablative Dose Yttrium-90 Radioembolization in Patients with Hepatocellular Carcinoma 5 cm or Larger. (Choi et al.) [<https://doi.org/10.1016/j.jvir.2023.10.011>]

RMSS Author: Salma Abosabie

RMSS Editors: Gabriel Knight, Julia D'Souza

SUMMARY (METHODS, RESULTS):

- This study assesses the safety and effectiveness of high-dose Yttrium-90 (Y-90) glass microsphere radioembolization in patients presenting with large hepatocellular carcinoma (HCC) **lesions measuring at least 5 cm in diameter**. Uniquely, the radioembolization approach in this study intentionally **preserves a small future liver remnant (FLR)**, targeting patients with large HCC of ≥ 5 cm requiring treatment for $>60\%$ of the total liver volume and having well-preserved liver function
- Researchers conducted a retrospective, single-center analysis involving 25 patients. All patients underwent ablative radioembolization using glass microspheres, with a mean absorbed dose of >150 Gy, and the FLR of nontumor liver volume (NTLV) was set at $>30\%$. Changes in liver function, adverse events, duration of response (DoR) in a treated area, time-to-progression (TTP), and overall survival (OS) were retrospectively investigated.

Key Findings:

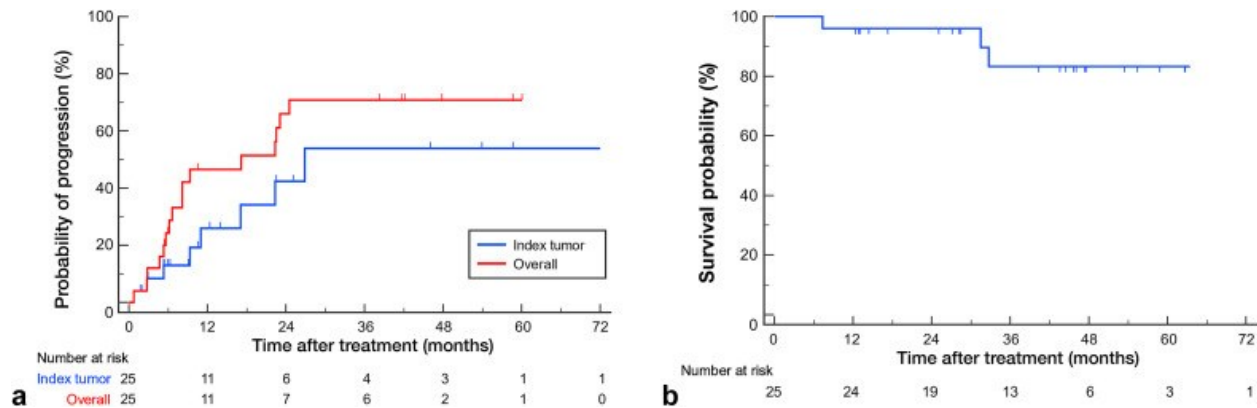
- The largest tumor diameter and planned dose per treated volume were $11.4 \text{ cm} \pm 3.9$ and $242.3 \text{ Gy} \pm 63.6$ ($169.4 \text{ Gy} \pm 45.9$ per whole liver volume), respectively.
- Among 25 patients undergoing ablative radioembolization for ≥ 5 cm HCC: liver disease was predominantly due to HBV (80%); all patients were Child–Pugh A and ECOG 0 (100%); ALBI grade was 1 in 68% and 2 in 32%; portal hypertension was present in 20%; mean MELD was 7.7 ± 1.8 .
- **Liver function stayed stable in all treated patients, with maintenance of Child-Pugh Class A status for a minimum of 90 days post-treatment.**
- **Adverse events were limited:** no cases of high-grade (3–4) hyperbilirubinemia or new ascites, and only one patient experienced treatable radiation pneumonitis.
- The most common side effects were mild (abdominal pain in 36% of cases and transient fever).
- Tumorous vs. nontumorous liver absorbed doses were $418.8 \text{ Gy} \pm 227.4$ and $69.0 \text{ Gy} \pm 32.1$, respectively (assessed via PET/CT or SPECT/CT)
- Effectiveness of high-dose Y-90 radioembolization:

- 36% complete response and 56% partial response (mRECIST criteria).
- Median duration of response (DoR) in treated areas was 22.0 months; median time-to-progression was 17.1 months.
- **Five-year overall survival rate reached 83.2%.**
- LR showed hypertrophy over 6 months, increasing safety margin post-procedure.
- Higher complete response was significantly associated with higher V100 (percentage of tumor receiving >100 Gy), higher tumor absorbed dose, and smaller tumor volume.

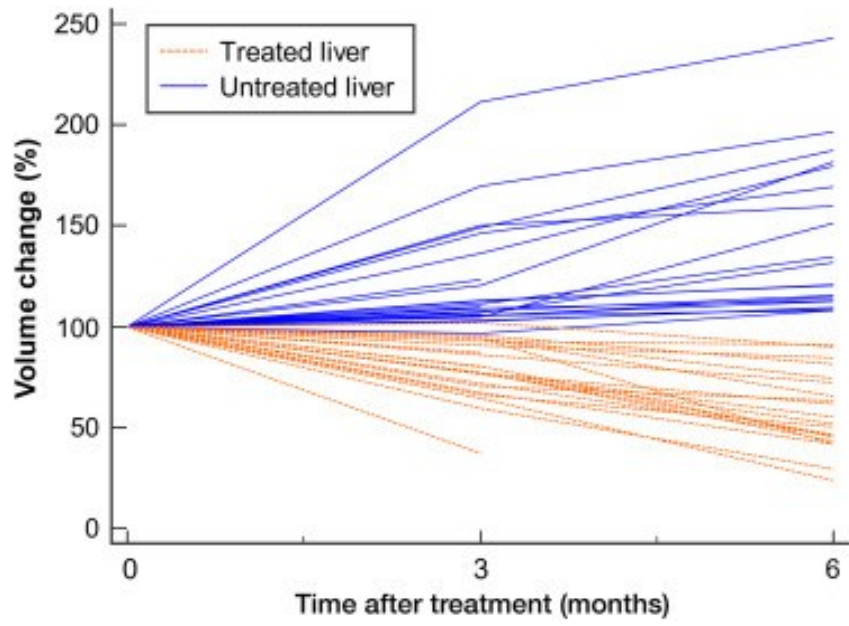
IMPORTANT TAKEAWAYS/DISCUSSION:

- **High-dose Y-90 radioembolization is feasible and well-tolerated in patients with large HCC who have preserved liver function**
- **Maintaining an FLR/NTLV ratio >30% is critical for safety**
- **Preserved liver function and minimal severe complications**
- **High objective response, durable disease control in treated liver, and excellent long-term survival**

KEY FIGURES:



Oncologic outcomes after radiation major hepatectomy of large hepatocellular carcinomas of ≥ 5 cm. (a) Time-to-progression (orange) and time-to-local-tumor progression (blue) of the index tumor (largest tumor). (b) Overall survival after radiation major hepatectomy.



Changes (%) in treated and untreated liver volumes after ablative radioembolization.

Paper #4: Locoregional Therapies for Hepatocellular Carcinoma prior to Liver Transplant: Comparative Pathologic Necrosis, Radiologic Response, and Recurrence. (Mosenthal et al.) [<https://doi.org/10.1016/j.jvir.2023.12.009>]

RMSS Author: Setayesh Sotoudehnia Korani

RMSS Editors: Gabriel Knight, Julia D'Souza

SUMMARY (METHODS, RESULTS):

- This was a single-center, retrospective study of 73 consecutive patients with solitary hepatocellular carcinoma (HCC) who received locoregional therapy (LRT) as a bridge or downstaging to liver transplant. Patients were treated with **transarterial chemoembolization (TACE) alone (n=14), yttrium-90 Y-90 radioembolization alone (n=36), or multimodal therapy (n=23, a pooled group of upfront combination therapies like TACE/ablation or therapy crossovers)**. The study compared **pathologic necrosis on the explanted liver, correlation with pre-transplant LI-RADS imaging response, and post-transplant tumor recurrence (median post-transplant follow-up time of 43 months)**.
- The results showed that **Y-90 alone and multimodal therapy achieved significantly greater pathologic necrosis compared to TACE alone (P=.01)**. The **highest rates of complete pathologic necrosis (CPN) were seen in TACE/ablation (71%) and high-dose Y-90 radiation segmentectomy (≥190 Gy) (63%)**. A **LI-RADS "nonviable" response was found to be an unreliable predictor of CPN**, with 75% sensitivity but low specificity (57%).

KEY FINDINGS:

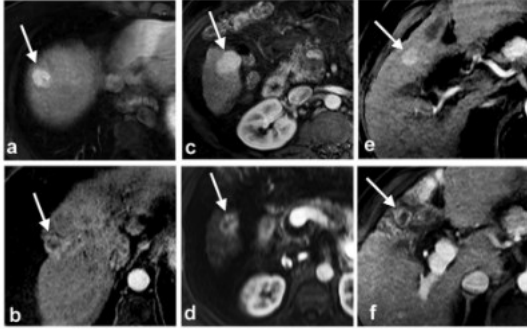
- **Pathologic Necrosis:**
 - **Y-90 alone and multimodal therapy were significantly superior to TACE alone (P=.01)**.
 - CPN rates by therapy:
 - TACE/ablation: 71% (n=5/7)
 - High-dose ^{Y-90} (≥190 Gy): 63% (n=17/27)
 - TACE alone: 21.4% (n=3/14)
- **Radiologic-Pathologic Correlation:**

- A LI-RADS "nonviable" response was **75% sensitive but only 57% specific for CPN.**
- The positive predictive value (PPV) of a "nonviable" response for CPN was 63%.
- **Tumor Recurrence:**
 - **Patients who achieved CPN had a 3% (1/36) recurrence rate.**
 - Patients without CPN had a 16% (6/37) recurrence rate.
 - This trend did not reach statistical significance (P=.11).
- **Other Factors:**
 - **Achieving CPN was associated with a smaller mean tumor size (2.5 cm vs. 3.2 cm for incomplete necrosis; P=.04).**
- **Safety profile**
 - No Grade 3 or higher procedure-related adverse events were observed.
 - Grade 3 or 4 laboratory toxicity (bilirubin and/or albumin) was identified in 4 of 73 patients (5%).
 - There was **no significant association between the type of LRT and the occurrence of laboratory toxicity.**

IMPORTANT TAKEAWAYS/DISCUSSION:

- **TACE alone was the least effective bridging therapy for achieving complete pathologic necrosis.**
- **High-dose ^{Y-90} radiation segmentectomy and multimodal therapy (especially TACE/ablation) were significantly more likely to achieve CPN** and had comparable results, supporting their use as "curative intent" bridging strategies.
- **Achieving CPN is associated with a strong trend toward lower post-transplant HCC recurrence, highlighting its importance as a therapeutic goal.**
- **Crucially, LI-RADS imaging criteria for "nonviable" tumor response is an unreliable predictor of CPN.** The high false-positive rate (low specificity) emphasizes that imaging alone cannot be used to confidently confirm complete tumor kill.

KEY FIGURES:



Axial MR images demonstrating the correlation (and lack thereof) between LI-RADS radiologic response and final explant pathology:

(a–b): A case where radiation segmentectomy resulted in a LI-RADS "nonviable" response that correctly matched complete pathologic necrosis at explant.

(c–d): A case treated with TACE showing a LI-RADS "viable" response which correctly matched incomplete necrosis (<50%) at explant.

(e–f): A critical example where a lesion treated with radiation segmentectomy showed an "equivocal" LI-RADS response (due to a ring of enhancement), yet explant pathology revealed complete pathologic necrosis. This highlights the study's finding that imaging does not always accurately predict the true extent of necrosis.

Paper #5: Radioembolization plus Immune Checkpoint Inhibitor Therapy Compared with Radioembolization plus Tyrosine Kinase Inhibitor Therapy for the Treatment of Hepatocellular Carcinoma. (Garcia-Reyes et al.)

[\[https://doi.org/10.1016/j.jvir.2024.02.004\]](https://doi.org/10.1016/j.jvir.2024.02.004)

RMSS Author: Gabriel Knight

RMSS Editors: Gabriel Knight, Julia D'Souza

SUMMARY (METHODS, RESULTS):

This retrospective, propensity score–matched cohort study compared outcomes of **yttrium-90 (Y-90) radioembolization combined with immune checkpoint inhibitor (ICI) therapy** versus **Y-90 combined with tyrosine kinase inhibitor (TKI) therapy** in patients with intermediate- to advanced-stage hepatocellular carcinoma (HCC). Forty-four patients treated within 4 weeks of systemic therapy initiation were analyzed: 19 patients (43.2%) with ICI (atezolizumab, bevacizumab, and tremelimumab, per STRIDE regimen) and 25 patients (56.8%) with TKI (sorafenib, lenvatinib, and erlotinib). The primary outcomes included imaging response, progression-free survival (PFS), overall survival (OS), and adverse events. The study found **significantly higher objective response and disease control rates with Y-90+ICI, fewer treatment-limiting adverse events with Y-90+ICI, and comparable survival outcomes, supporting the safety and potential efficacy advantages of combining Y-90 with immunotherapy.**

Key Findings:

- In both groups: the etiology of HCC was predominantly Hepatitis C infection (68% of patients in the 90Y+TKI group; 53% in the 90Y+ICI group); patients primarily presented with Child–Pugh A (100% Child–Pugh A in the ICI group; 89% in the TKI group), and BCLC Stage C (76% in the TKI group; 79% in the ICI group) tumors, most commonly due to macrovascular invasion.
- Patients in the **Y-90 plus ICI therapy group had better objective response rates (ORRs) (89.5% vs 36.8%; $P < .001$) and disease control rates (DCRs) (94.7% vs 63.2%; $P < .001$) than those receiving Y-90 plus TKI** by both mRECIST and iRECIST criteria (ORR: 78.9% vs 36.8%; $P < .001$; DCR: 94.7% vs 63.2%; $P < .001$).
 - This benefit was observed for both index lesions and overall tumor burden.
- Median overall survival (15.8 vs 14.3 months) and progression-free survival (8.3 vs 4.1 months) were numerically longer with Y-90+ICI but did not reach statistical

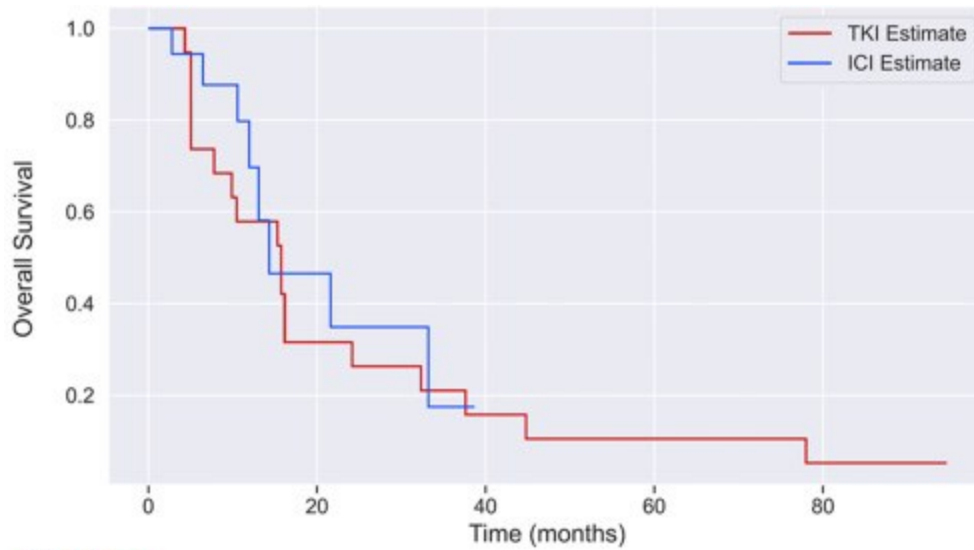
significance on Kaplan-Meier analysis, possibly secondary to limited sample size and censoring in the ICI cohort.

- Only 5.3% of patients in the Y-90+ICI group discontinued systemic therapy due to adverse effects, compared with 63.2% in the Y-90+TKI group. **Overall adverse event burden was significantly lower with ICI-based therapy.**
- **No treatment-limiting adverse events were attributed to Y-90 radioembolization in either cohort.** Radiation-related toxicities were limited to mild transient symptoms (Grade 1 fatigue, nausea, or abdominal pain) with no subsequent complaint at follow-up, supporting the procedural safety of Y-90 in combination systemic regimens.

IMPORTANT TAKEAWAYS/DISCUSSION:

- The substantially **higher ORR and DCR with Y-90+ICI suggest a meaningful synergistic interaction between radioembolization and immunotherapy**, potentially mediated by enhanced tumor immunogenicity following radiation-induced cell death. This effect was durable across both conventional and immune-specific response criteria.
- Despite improved imaging response, survival differences were not statistically significant, likely due to small sample size, retrospective design, and heavy censoring of the more recently treated ICI cohort. Multivariable Cox regression, however, did identify ICI use as independently associated with longer PFS.
- **ICI-based regimens were far better tolerated than TKIs**, with fewer grade ≥ 3 toxicities and markedly fewer therapy discontinuations. This improved tolerability may translate into better adherence, longer systemic treatment duration, and improved quality of life for patients with advanced HCC.
- These findings support **Y-90 radioembolization as a safe and effective adjunct to modern immunotherapy regimens in intermediate- to advanced-stage HCC**. While randomized trials are needed, the data reinforce a growing **paradigm shift away from TKI-based combinations toward immunotherapy-centered multimodal treatment strategies**.

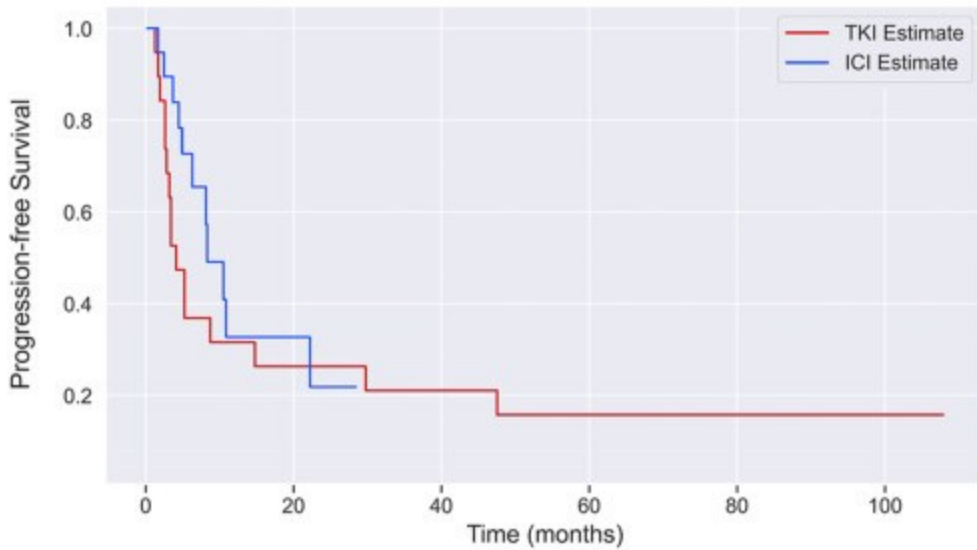
KEY FIGURES:



TKI Estimate					
At risk	19	6	3	2	1
Censored	0	0	0	0	0
Events	0	13	16	17	18

ICI Estimate					
At risk	19	4	0	0	0
Censored	0	9	11	11	11
Events	0	6	8	8	8

a



TKI Estimate					
At risk	19	5	4	3	1
Censored	0	0	0	0	2
Events	0	14	15	16	16

ICI Estimate					
At risk	19	3	0	0	0
Censored	0	6	8	8	8
Events	0	10	11	11	11

b

(a) Overall survival and (b) progression-free survival curves after propensity matching for patients receiving Y-90 and systemic therapy.

Paper #6: Track Sealing in CT-Guided Lung Biopsy Using Gelatin Sponge Slurry versus Saline in Reducing Postbiopsy Pneumothorax: A Prospective Randomized Study. (Dheur et al.) [<https://doi.org/10.1016/j.jvir.2024.07.019>]

RMSS Author: Gabriel Knight

RMSS Editors: Gabriel Knight, Julia D'Souza

SUMMARY (METHODS, RESULTS):

High Level Summary

- This prospective randomized study compared two track sealing techniques following CT-guided lung biopsy - **gelatin sponge slurry (GSS)** versus **saline** - to determine their effectiveness at reducing postbiopsy pneumothorax. 266 patients undergoing lung biopsy were randomized to receive either GSS or saline sealing. The **primary outcome** was pneumothorax incidence; secondary outcomes included **intervention rates** for pneumothorax and **hospital length of stay**. The study showed that **GSS track sealing significantly reduced pneumothorax rates and shortened hospital stays** versus saline, with emphysema identified as a risk factor for pneumothorax.

Key Findings:

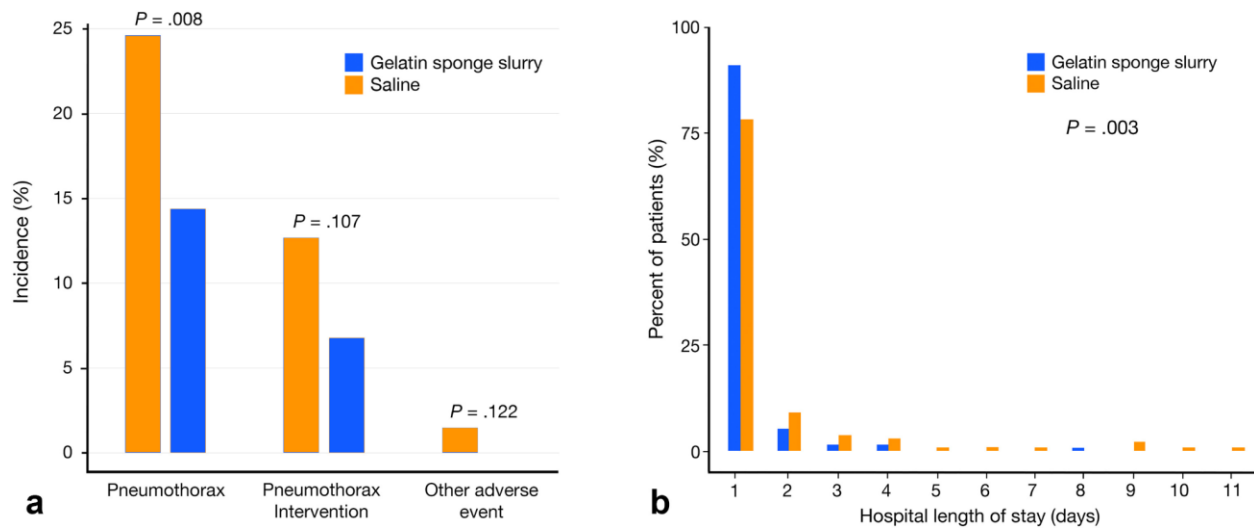
- The **pneumothorax rate was significantly lower in the GSS group** (12.1%) compared with the saline group (24.6%), indicating that sealing the biopsy track with GSS effectively reduces postbiopsy pneumothorax risk.
- Patients treated with **GSS had a significantly shorter hospital length of stay** compared to those receiving saline sealing, suggesting clinical and logistical benefits.
- Although fewer GSS patients required pneumothorax-related intervention (i.e. simple aspiration or drainage) – specifically, 9 patients (6.8%) in the GSS group compared to 17 patients (12.7%) in the saline-sealing group – the difference did not reach statistical significance (6.8% vs 12.7%).
- In multivariable analysis, GSS was protective (odds ratio ~0.44) against pneumothorax, while **emphysema significantly increased pneumothorax risk**.

IMPORTANT TAKEAWAYS/DISCUSSION:

- Using GSS for track sealing after CT-guided lung biopsy can meaningfully reduce pneumothorax incidence, one of the most common complications of percutaneous lung biopsy. This technique may improve patient safety and reduce the need for postbiopsy care resources.

- Shorter hospital stays with **GSS tract-sealing may translate to cost savings and improved throughput** in high-volume centers performing lung biopsies. Fewer pneumothoraces also may reduce downstream interventions and patient discomfort.
- Although GSS was protective overall, **patients with preexisting emphysema remained at higher risk for pneumothorax**, underscoring the **importance of individualized risk assessment in procedural planning**.
- Given the growing emphasis on minimizing procedural complications, these results support wider adoption of GSS sealing techniques and may prompt further research comparing alternative sealants and protocols.

KEY FIGURES:



Histograms displaying (a) incidences of adverse events and (b) length of hospital stay in days for each group.

Paper #7: Radiofrequency Ablation in Patients with Interstitial Lung Disease and Lung Neoplasm: A Retrospective Multicenter Study. (Yamamoto et al.)

[\[https://doi.org/10.1016/j.jvir.2024.06.010\]](https://doi.org/10.1016/j.jvir.2024.06.010)

RMSS Author: Chris Hsu

RMSS Editors: Gabriel Knight, Julia D'Souza

SUMMARY (METHODS, RESULTS):

- This retrospective, multicenter study investigates the **safety and effectiveness of percutaneous radiofrequency ablation (RFA) in patients with lung neoplasm and concomitant interstitial lung disease (ILD)**, a population at high risk for treatment-related pulmonary complications.
- 49 patients with ILD and 64 lung neoplasms were treated in 66 RFA sessions. 23 (47%) patients had usual interstitial pneumonia on CT.
- Key adverse events measured included pneumothorax, pleural effusion, acute ILD exacerbation, or other events resulting in unplanned increase in care, hospitalization, disability, or death.
- Key outcomes included overall survival (OS), local tumor progression (LTP), and median survival time.

Key Findings:

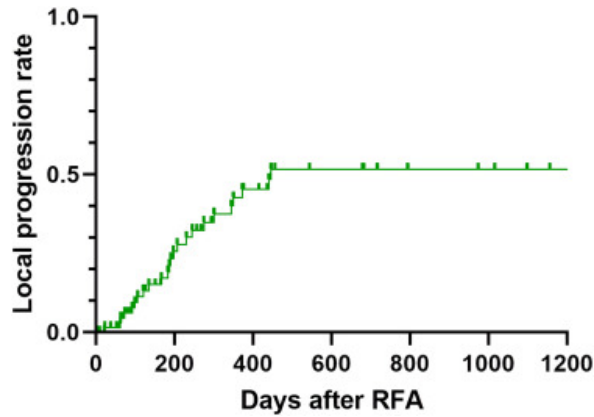
- **RF ablation achieved a 100% technical success rate in patients with ILD**, including nearly half with a UIP pattern. However, the procedure carried a **risk of delayed acute ILD exacerbation, underscoring that feasibility does not equate to low clinical risk in this population.**
 - Acute exacerbation of ILD occurred in 5 of 66 sessions (8%), with symptom onset ≥ 8 days post-procedure (median 12 days). **60% percent of affected patients (n = 3) died, corresponding to a 5% per-session mortality**, substantially higher than RF ablation mortality in patients without ILD.
- **Pleural effusion and fever after RFA were identified as significant risk factors for acute exacerbation**
- Overall Survival (OS)
 - 1-year OS: 83%
 - 3-year OS: 62%
 - 5-year OS: 36%
- Local tumor Progression (LTP)

- 1-year LTP: 43%
- 3-year LTP: 52%
- Median survival time: 45.3 months

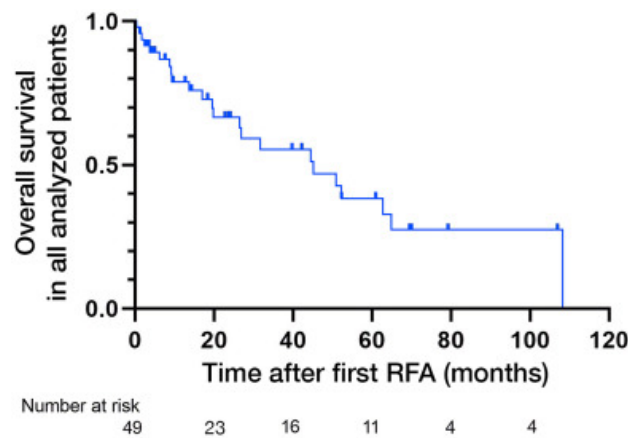
IMPORTANT TAKEAWAYS/DISCUSSION:

- **While RFA demonstrated technical feasibility as a treatment option for lung neoplasms in ILD patients, there is a risk of delayed acute exacerbation possibly leading to death, which should be part of pre-procedure counseling.**
- Local progression rates of tumor were higher than previous reports at 1 year (43% vs 4 - 31.1%), possibly due to insufficient ablation margins secondary to avoidance of adverse events as an operator.
 - This highlights a **critical trade-off in ILD patients: aggressive ablation may improve oncologic control but at the cost of increased, potentially fatal pulmonary complications**
- Unlike surgical exacerbations that typically occur early, **ILD exacerbations after RF ablation were consistently delayed beyond 1 week.** This delay highlights the **need for extended clinical monitoring, particularly in patients who develop postprocedural fever or pleural effusion,** even if early recovery appears uneventful.
- Limitations of the Study
 - Retrospective design
 - Diagnosis of ILD was not based on pathological findings and ILD status was not confirmed via imaging unless diagnosis was already present
 - The study included primary and metastatic lung neoplasms, limiting comparison to other studies
 - More than half of the neoplasms were not diagnosed by biopsy to avoid risks involved in patients with ILD. However, tumor type was not considered related to the risk of RFA in the study
 - Lack of multivariate analysis for confounders with a modest sample size that does not fully stratify for how severity or functional status affects outcomes

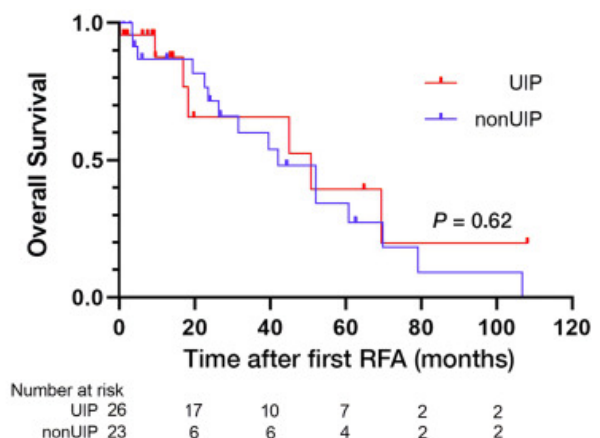
KEY FIGURES:



Cumulative local tumor progression rate of ablated tumor after lung radiofrequency (RF) ablation in all 64 tumors. Cumulative local tumor progression rates were 43% at 1 year and 52% at 3 years.



a Survival results. (a) Cumulative survival rate after lung radiofrequency (RF) ablation in 49 patients. One-, 3-, and 5-year survival rates were 83%, 62%, and 36%, respectively. Median survival time was 45.3 months. (b) Cumulative survival rate after lung RF ablation was 50.9 months in patients with a usual interstitial pneumonia (UIP) pattern (UIP with red line) on computed tomography (CT) and 42.2 months in patients without a UIP pattern (non-UIP). No significant difference was evident ($P = .62$).



Paper #8: Embolization of the Pancreas Using Microspheres: A Proof-of-Safety Study in a Porcine Model. (Cline et al.) [<https://doi.org/10.1016/j.jvir.2024.06.034>]

RMSS Author: Katrina Falk

RMSS Editors: Gabriel Knight, Julia D'Souza

SUMMARY (METHODS, RESULTS):

- Concern for acute pancreatitis after particle-based transarterial embolization has limited its preclinical and clinical study. However, **recent retrospective data has shown that embolization with coils or glue for pancreatic hemorrhage did not cause pancreatitis.**
- This proof-of-safety preclinical study evaluated **particle embolization of the pancreas** using 100–300 µm microspheres in a porcine model to assess feasibility, pancreatic injury, and endocrine/exocrine function.
- Fourteen pigs underwent selective embolization of the dorsal pancreatic artery and were **monitored for 2 weeks with serial pancreatic enzyme testing, glucose tolerance testing, and behavioral observation**; necropsy and pathology evaluation was performed following euthanasia 2 weeks post-embolization.
- All embolizations were technically successful, and no animals developed clinical pancreatitis or distress.
- **Although pancreatic enzymes rose transiently, all normalized by 2 weeks.**
- Histopathology showed localized ischemic fibrosis without active inflammation.
- The study suggests that **small-particle pancreatic embolization may be well-tolerated without clinically-significant pancreatitis or loss of pancreatic function.**

Key Findings:

- Serum amylase and lipase transiently increased from 1780.4 µg/mL and 5.7 µg/mL at baseline to 9139 µg/mL and 448.4 µg/mL at 24 hours and 6830.4 µg/mL and 281.1 µg/mL at 48 hours, respectively. **Both returned to baseline after 2 weeks**, noting that it was not explicitly specified whether additional treatment/fluids were provided in these subjects.
- Insulin and glucose levels after a glucose tolerance test were **similar before and after embolization with the only statistical difference occurring at 2 and 5 minutes post glucose administration.**
- On gross necropsy, ~25% of the pancreas was noted to be ischemic.

- Histologically, there was complete loss of normal pancreatic architecture with loss of acinar cells, lack of islet structures and replacement by fibrous connective tissue with extensive angiogenesis, admixed chronic inflammatory cells and extensive pancreatic ductal proliferation within the embolized area. Inflammatory cells consisted mostly of lymphoid cells with scattered pigment-laden (hemosiderin) macrophages. There were sharply demarcated borders between the embolized tissue and adjacent normal pancreatic acinar tissue.

IMPORTANT TAKEAWAYS/DISCUSSION:

- Particle embolization of the pancreas was feasible and tolerated in this in vivo swine model
- Despite deliberate ischemia and small-particle embolization, **clinically significant pancreatitis did not occur**. The absence of ductal injury, limited inflammatory response, and lack of reperfusion injury may explain why **pancreatic necrosis and fibrosis did not translate into symptomatic pancreatitis** in this model.
- Even with destruction of both acinar and islet cells in embolized regions, overall pancreatic function remained intact. These findings suggest that **partial pancreatic embolization may be feasible without inducing diabetes or malabsorption**, provided embolized volume remains limited.
- The study supports the biological **plausibility of transarterial embolization strategies for pancreatic tumors**, particularly hypervascular neoplasms or as adjunctive intra-arterial therapies. It also reinforces prior clinical observations that pancreatic embolization for hemorrhage is often well tolerated.
- Limitations of this study's generalizability include **embolization of only the dorsal pancreatic artery**, which supplies ~32% of the total porcine pancreas and has a different configuration compared to humans

KEY FIGURES:

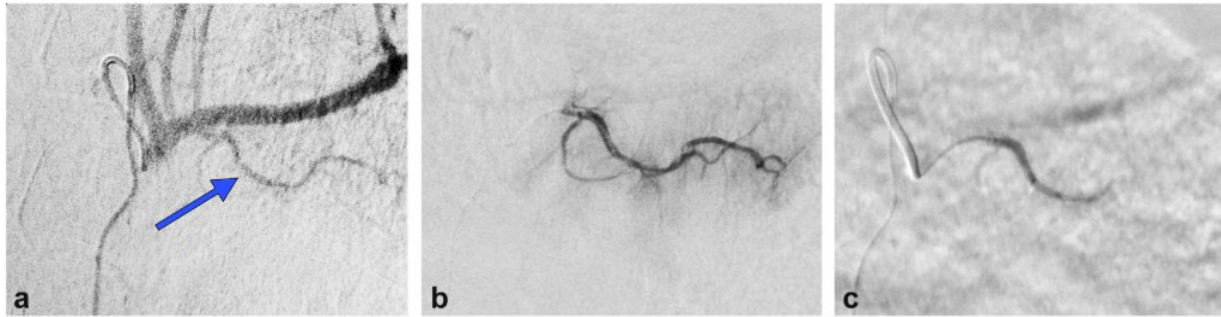


Figure 2. (a) Celiac arteriogram demonstrating the dorsal pancreatic artery (blue arrow), (b) dorsal pancreatic arteriogram via microcatheter before embolization, and (c) stasis in the dorsal pancreatic artery following embolization.

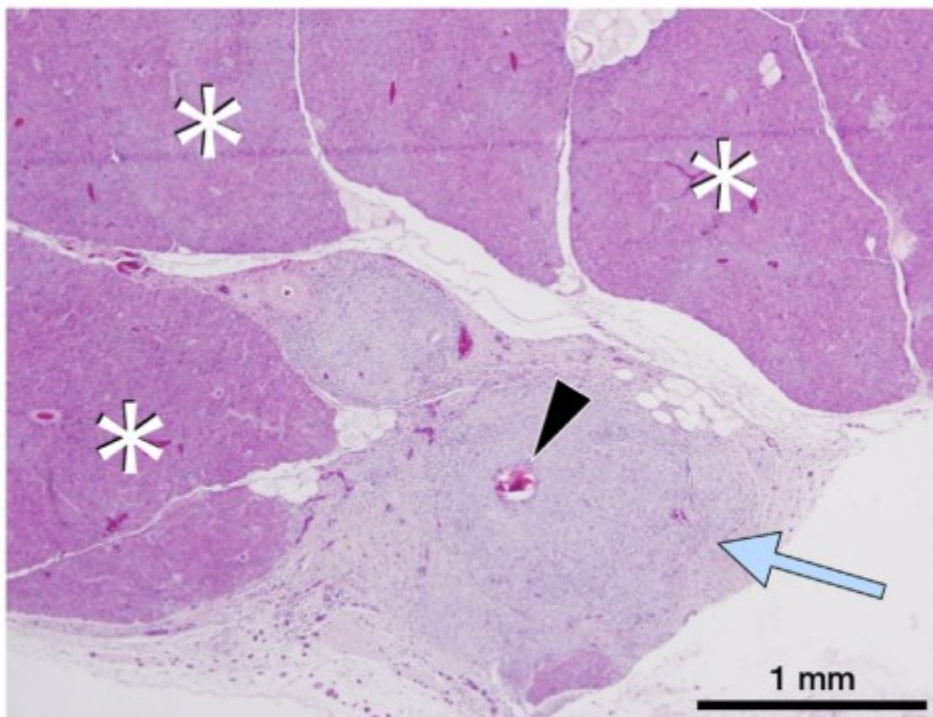


Figure 6. Micrograph of pancreatic tissue at the margin between the normal and embolized pancreas. Fibrofatty-replaced pancreatic tissue without active inflammation (light blue arrow) immediately adjacent to normal-appearing pancreas (asterisks), without evidence of inflammation. Black arrowhead, embolic microsphere within a capillary inside the embolized portion.